Journal of Microbiological Methods 159 (2019) 200–210

Contents lists available at ScienceDirect

Journal of Microbiological Methods

journal homepage: www.elsevier.com/locate/jmicmeth

Novel biocompatible poly(acrylamide)-grafted-dextran hydrogels: Synthesis, characterization and biomedical applications

Sudha B. Patil[a], Syed Z. Inamdar[a], Kakarla Raghava Reddy[b], Anjanapura V. Raghu[c,d], Sarvesh K. Soni[e], Raghavendra V. Kulkarni[a,*]

[a] Department of Pharmaceutics, BLDEA's SSM College of Pharmacy and Research Centre, Vijayapur 586 103, Karnataka, India
[b] School of Chemical and Biomolecular Engineering, The University of Sydney, Sydney, NSW 2006, Australia
[c] Department of Basic Sciences, School of Engineering & Technology, JAIN Deemed-to-be University, Bangalore 562112, Karnataka, India
[d] Food Technology, Centre for Emerging Technology, JAIN Deemed-to-be University, Bangalore 562112, Karnataka, India
[e] School of Sciences, RMIT University, Melbourne 3001, Australia

ARTICLE INFO

Keywords:
Bio-nanotechnology
Polymer hydrogel
Grafting
Antibacterial
Transdermal drug delivery
Rivastigmine tartarate

ABSTRACT

An electro-responsive PAAm-g-Dxt copolymer was synthesized and characterized by ^{1}HNMR & FTIR spectroscopy, neutralization equivalent, elemental and thermogravimetric analysis to ascertain the grafting reaction. Further, we developed an electro-responsive transdermal drug delivery system (ETDS) utilizing PAAm-g-Dxt copolymer for rivastigmine tartarate delivery through skin. The ETDS were developed using drug-loaded PAAm-g-Dxt hydrogel as the reservoir, and cross-linked dextran-poly(vinyl alcohol) blend films as rate controlling membranes (RCM). In the absence of electrical stimuli, a small amount of drug was permeated from the ETDS, while in the presence of electrical stimuli, the drug permeability was increased. On application of electric stimulus, the flux was increased by 1.6 fold; drug permeability was enhanced when the strength of applied electric current was raised to 8 mA from 2 mA. The drug permeability characteristics studied under "on–off" stimuli suggested that there was faster drug permeation when electrical stimuli was 'on' and it decreased when electrical stimuli was 'off.' The histopathology study confirmed the altered skin structural integrity after application of electrical stimuli. Hence, the PAAm-g-Dxt based ETDS are useful for transdermal drug delivery triggered by an electric stimulus to deliver on-demand release of drug into systemic circulation.

1. Introduction

A three-dimensional, hydrophilic, polymer network structure having an efficiency to absorb a huge quantity of body fluids or water is termed as Hydrogel (Peppas and Merrill, 1976a). The homopolymers or copolymers are the building blocks of the hydrogel network structure and are either cross linked chemically or physically and render it insoluble and provide structural and physical integrity (Peppas and Merrill, 1976b; Stauffer and Peppas, 1992; Hickey and Peppas, 1995; Peppas and Mongia, 1997). The hydrogels tends to swell when bought in contact with water, thus revealing a thermodynamic compatibility in aqueous medium (Flory and Rehner, 1943; Flory, 1950; Ratner and Hoffman, 1976). In comparison to other available synthetic biomaterials, hydrogels bear more resemblance to natural living tissue owing to their greater softness consistency and water content akin to natural tissue (Peppas and Langer, 1994). Further, the superior water content property of the hydrogel biomaterial enhances its biocompatibility and has a profound use in contact lenses, biosensor membranes, materials for artificial hearts, skin, and drug delivery devices (Peppas, 1997).

A strong cholinesterase inhibitor like rivastigmine needed only in tiny dose for an effective treatment is chemically an ideal candidate suitable for transdermal delivery. Rivastigmine has a smaller molecular size (< 500 Da) and is both hydrophilic and lipophilic in nature and can readily pass into the systemic circulation through skin, hence, it can be a patch deliverable medicine with the feasibility to prepare the patch as small and discrete (Birks et al., 2000). This will improve adhesion and minimize untoward frequent risk of adverse skin effect.

The degree of adverse effect akin to oral delivery of drugs can be overcome by transdermal drug delivery approach, where the drug's active component are delivered through the skin with the advantage of having sustained drug release and optimum strength of action. Transdermal dosage forms of drugs are self-contained and discrete. Most of the drugs do not reaches the targeted area in the body with adequate concentration so as to elicit therapeutic response because

* Corresponding author.
E-mail address: pharma_75raghu@yahoo.com (R.V. Kulkarni).

https://doi.org/10.1016/j.mimet.2019.03.009
Received 21 January 2019; Received in revised form 10 March 2019; Accepted 11 March 2019
Available online 12 March 2019

many of them are prematurely excreted or inactivated in conventional drug delivery system. TDDS reduces the dosing frequencies of drug by delivering the drugs directly into the intended site of action that's why less amount of dose of drug is required (Gorle, 2016; Manikkath et al., 2017).

The physicochemical properties of natural and synthetic polymers can be modified without significantly affecting its basic properties by using a technique called Graft copolymerization (Chauhan et al., 2010). Usually grafting results from the radical sites generated on the polymer backbone through propagation. Various studies have been reported for the preparation polymeric material through graft copolymerization of monomers onto natural polymers (Sharma and Mishra, 2010; Kumari et al., 2010). Chemically altering starch to enhance its properties was brought about by vinyl graft *co*-polymerization. This was an effective method to improve and broaden the scope and degree of starch utilization. Natural polymers can be improvised of their characteristics through the technique of Polymer grafting. The resulting graft polymers can be made into ionic copolymers with pH- sensitive characteristics by the hydrolysis of the amide group; such polymeric property can be effectively utilized for targeted drug delivery approaches. Also, the matrix of grafted polymer tends to posses enhanced free volume which eventually increases the drug loading capacity (Boppana et al., 2016).

Dextran, is a polysaccharide with the composition of α-1,6-linked D-glucopyranose units. It is biocompatible, biodegradable, and possesses large number of hydroxyl groups on its backbone, and those could be easily subjected for functional modification to get desired properties. It is a widely chosen polysaccharide for the development of hydrogels in biomedical applications, like drug delivery (Hennik et al., 2004), scaffolds for tissue engineering (Le'Vesque et al., 2005) and antibacterial polymer (Bankova et al., 1997; Oh et al., 1996). The antibacterial polymers usually obtained either by synthesis of monomeric biocide moiety and subsequent polymerization or copolymerization with another monomer or modification can also be brought by grafting of *N*-alkylated poly (4-vinylpyridine) quarternized polyethylenimine and quaternary derivatives of acrylic acid onto numerous materials such as celluloses etc. (Lee et al., 2004; Tiller et al., 2002).

An antibacterial property of dextran was reported through lysozyme-dextran conjugation; results showed an improved antibacterial activity with an increased enzyme-conjugate concentration. This conjugate was effective against *E. coli* (Amiri et al., 2008). In another study, *N*-succinyl chitosan was used to prepare antibacterial dextran/chitosan hydrogel as a postsurgical aid in endoscopic sinus surgeries and it has shown excellent antimicrobial properties, the antibacterial activity was not due to the *N*-succinyl chitosan component of the gel, but it was due to dextran (Aziz et al., 2012).

The objective of current study was to develop an electro-responsive transdermal delivery system (ETDS) for on-demand delivery of rivastigmine tartarate using polyacrylamide-g-dextran (PAAm-g-Dxt). The PAAm grafting on Dxt was carried out and further the amide (–$CONH_2$) groups of PAAm part were transformed into –COONa. This PAAm-g-Dxt copolymer hydrogel was employed as drug reservoir and cross-linked blend films of Dxt and PVA were acted as rate controlling membranes to fabricate ETDS. The in-vitro drug diffusion across rat skin was estimated in the presence or absence of an electrical current.

2. Materials and methods

2.1. Materials

Rivastigmine tartarate gift sample was requested and received from Sun Pharmaceutical Ltd., India.Dextran, ammonium persulfate, acrylamide, and methanol were procured from HiMedia Ltd. (Mumbai, India). Sodium hydroxide was procured from CDH Fine chemicals (Mumbai, India). Methyl paraben was procured from Nice chemicals (Mumbai, India). Glutaraldehyde (25% *w/v*), polyvinyl alcohol and hydrochloric acid were procured from SD Fine Chemicals (Mumbai, India). Polyethylene glycol 200 was procured from Loba Chemie Ltd. (Mumbai, India). For the whole work, condensed water was employed.

2.2. Synthesis of electro-responsive polyacrylamide-g-dextran graft copolymer

A free radical polymerization approach was used to prepare the graft copolymer of Dextran (Dxt) and acrylamide (AAm) (Kulkarni and Sa, 2008). In a 100 ml of double distilled water; two gm of Dxt was dissolved under nitrogen atmosphere. The Dxt solution was heated upto 80 °C and to this ammonium persulphate (0.43 g) was added. After 20 min, 10 ml of 0.105 mol AAm was added and reaction was allowed for 60 min with nitrogen environment. After 60 min, the resulting copolymer was kept to cool down to room temperature and later mixed with 400 ml methanol, the product was repeatedly washed with methanol and finally the copolymer product was allowed to dry at 50 °C for the night and then percent grafting efficiency and AAm grafting were calculated as follows.

$$\text{Percent AAm grafting} = \frac{\text{Mass of AAm in grafted polymer}}{\text{Mass of the grafted polymer}} \times 100 \quad (1)$$

$$\text{Percent grafting efficiency} = \frac{\text{Mass of grafted polymer-Mass of Substrate}}{\text{Mass of monomer}} \times 100 \quad (2)$$

The PAAm-g-Dxt was subjected to alkaline hydrolysis using sodium hydroxide. In a 100 ml sodium hydroxide (0.9 M), an accurately weighed quantity (2 g) of graft copolymer was mixed. The solution was maintained at a temperature of 75 °C in thermostatic water bath and stirred at 100 rpm for 60 min till the completion of hydrolysis reaction. The solution was poured into 400 ml methanol after cooling it to room temperature. The copolymer then dried overnight at 50 °C and stored in moisture free container.

2.3. Characterization of PAAm-g-Dxt copolymer

2.3.1. Proton nuclear magnetic resonance (^{1}HNMR) analysis

The proton NMR studies were carried out on native Dxt, PAAm-g-Dxt and acrylamide. Internal standard used was tetramethylsilane (TMS). After samples were dissolved in dimethylsulfoxide (10 mg/dm^3) at 60 °C, spectral derivation was performed using Varian Spectrophotometer (Mercury Plus 300 MHz NMR, WA, USA).

2.3.2. Fourier transform infrared spectroscopy

A FTIR analysis of the copolymer was performed to confirm grafting and hydrolysis reaction. Samples of the copolymer were compressed along with potassium bromide at 600 kg pressure to prepare thin pellets. Then the pellets were scanned at 2 cm^{-1} resolution with 64 scans in the range between 500 and 4000 cm^{-1} to obtain spectra using FTIR instrument (8400S, Shimadzu, Japan).

2.3.3. Determination of neutralization equivalent (NE)

An equivalent weight of acid which can be determined by titration against standard alkali is termed neutralization equivalent (Tripathy and Singh, 2000). A 200 mg copolymer was soaked in 0.1 N HCl for about six hours, then the excess hydrogen ion concentration was estimated by back titration using 0.1 N sodium hydroxide.

2.3.4. Elemental analysis

An Elemental analysis was performed to estimate and calculate the percent of nitrogen, carbon and hydrogen for native Dxt, PAAm-g-Dxt and Hydrolyzed PAAm-g-Dxtusing a CHN analyzer (Exeter Analytical, Chelmsford, MA).

2.3.5. Thermogravimetric analysis (TGA)

A microcalorimeter (Diamond TG/DTA, Perkin Elmer, USA) was

Table 1
Formulation details of electrically responsive transdermal systems.

Code	Hydrogel reservoir					Rate controlling membranes				
	PAAm-g-Dxt (%*W/V*)	Rivastigmine tartarate (%*w/w*)[a]	GA (% w/w)[a]	0.1 N HCL (ml)	Methyl paraben (mg)	Dextran (% *w/v*)	Polyvinyl alcohol (% w/v)	Polyethylene glycol 200 (% w/w)	GA (% w/w)[a]	0.1 N HCl (ml)
Dxt 1	3	20	3	0.5	15	2	2	10	3	0.5
Dxt 2	4	20	3	0.5	15	2	2	10	3	0.5
Dxt 3	5	20	3	0.5	15	2	2	10	3	0.5
Dxt 4	5	20	6	0.5	15	2	2	10	3	0.5
Dxt 5	5	20	9	0.5	15	2	2	10	3	0.5
Dxt 6	5	20	9	0.5	15	2	2	10	6	0.5
Dxt 7	5	20	9	0.5	15	2	2	10	9	0.5
Dxt 8	5	20	9	0.5	15	2	2	10	12	0.5

[a] %w/w of polymer.

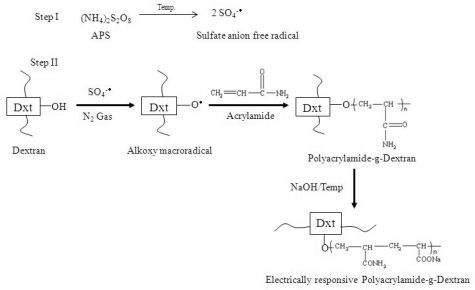

Scheme 1. Scheme for synthesis of electrically-responsive PAAm-g-Dxt graft copolymer.

employed for TG analysis of Dxt and PAAm-g-Dxt under dynamic argon gas at the rate of 50 ml/min and 10 °C /min between 30 and 600 °C.

2.4. Formulation of electrically-responsive transdermal drug delivery systems

Formulation of electro-responsive transdermal delivery systems (ETDS) involves two parts i.e., preparation of electro-responsive hydrogel reservoir and preparation of rate controlling membranes (RCM).

2.4.1. Preparation of hydrogel reservoir

The electro-responsive hydrogel reservoir was developed by mixing exactly weighed quantity of PAAm-g-Dxt in purified water. The homogenous polymeric solution was obtained with continuously stirring on magnetic stirrer. The accurately weighed amounts of methyl paraben and drug were mixed with the above solution and then the glutaraldehyde (GA) along with 0.1 N HCl (0.5 ml) were added and stirred for half an hour. Thus prepared hydrogel reservoir was preserved in a air tight container for preparing ETDS (Table 1).

2.4.2. Preparation of rate controlling membranes

The RCMs were prepared by glass plate method. The native Dxt and polyvinyl alcohol (PVA) were allowed to dissolve in purified water to obtain homogeneous solution. The GA and 0.1 N HCl along with polyethylene glycol 200 (PEG 200) were mixed with the above solution with stirring; then this polymeric solution was transferred into glass bangle fixed on glass plate which in turn placed on mercury and left for 48 h. Then the dried membranes were taken out and stored in a desiccator. The composition is given in Table 1.

Further, ETDS were prepared using polystyrene backing film, on which a precisely weighed quantity of hydrogel reservoir was placed, further RCM was positioned above the hydrogel and the circumference was sealed to make it leak-proof; they were stored in a well closed container for evaluation (Mutalik and Udupa, 2005).

2.5. Evaluation of electro-responsive transdermal systems

2.5.1. Evaluation of hydrogel reservoir

2.5.1.1. Drug content. An accurately weighed quantity of PAAm-g-Dxt reservoir hydrogel (1 g) was dissolved in 80 ml of pH 7.4 buffer and kept for 12 h. The obtained solution was gently heated at 40 °C for 10 min and cooled to room temperature. The solution was filtered and made up to a final volume of 100 ml using pH 7.4 buffer before measuring the absorbance at 264 nm in UV-VIS spectrophotometer (UV-1800, Shimadzu, Japan).

2.5.1.2. Determination of pH. Accurately weighed amount of reservoir hydrogel (1 g) was added to 10 ml of double distilled water and pH was measured using pen pH meter.

2.5.2. Evaluation of rate controlling membranes

2.5.2.1. Thickness uniformity. The thickness of RCMs was calculated using Digital micrometer (Mitutoyo, Japan) at three different places and average of the three observations was presented.

2.5.2.2. Water vapor transmission (WVT) studies. This study employs equal diameter glass vials as transmission cells. To the washed and oven dried cells, the two gm of fused calcium chloride was placed inside cells and the brim was fixed with RCM using an adhesive. These cells are precisely weighed initially and recorded before keeping them in closed desiccator containing a saturated potassium chloride solution (500 ml) for a period of 24 h with a defined humidity of 84% RH. The cells were removed at different time intervals for 24 h and weighed to calculate the rate WVT using the equation.

$$WVT = WL/S \quad (3)$$

where, W = Grams of water vapors transmitted, L = Film thickness in cm, S = Surface area in cm^2.

2.5.2.3. Tensile strength. Universal testing machine (Hounsfield, Slinfold, Horsham, U.K.) was employed to measure tensile strength, which posses two load cell jaws; of which, one is movable (upper) and the other is fixed (fixed). Rectangular RCMs of 2 × 0.8 cm^2 sizes were cut and deployed to measure tensile strength. The RCM was placed and fixed between cell jaws, where the upper jaw was moved steadily till the RCM was broken at a speed of 100 mm/min (ISI Standard speed) with applied force using 10 kg load cell. The tensile strengths were recorded directly from the dial in kilograms and extension value in mm.

2.5.2.4. Scanning electron microscopy. The RCMs were coated with platinum using sputter coater (Edward S 150, UK) after mounting on the stubs. Then the films were examined under scanning electron microscope (JEOL, JSM-6360, Kyoto and Japan) at 10 kV and suitable magnification.

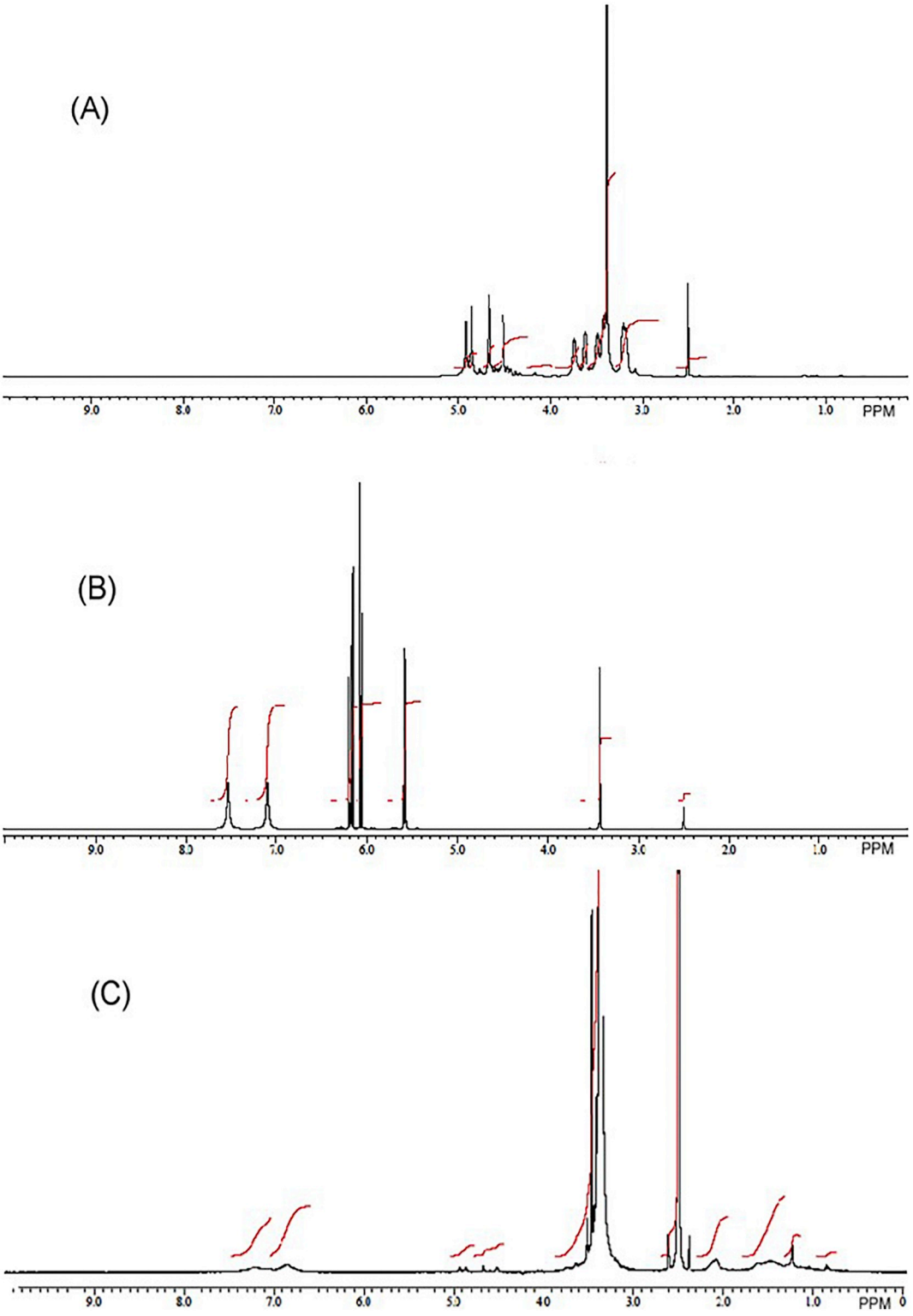

Fig. 1. ^{1}HNMR spectra of Dxt (A), AAm (B) and PAAm-g-Dxt (C).

2.5.2.5. Differential scanning calorimetry. The DSC analysis of RCM was carried out by recording thermograms at a heating rate 10 K/min from 20 °C to 300 °C temperature used under nitrogen flow of 25 ml/min. The samples were sealed in aluminum crucibles with the lid perforated prior to the test. For reference empty aluminum crucible was used.

2.5.2.6. X-ray diffraction. The Philips, PW -171, X-ray diffractometer was used for recording difractograms using quartz as internal standard. The diffractometer was connected to a digital graphical assembly and then computer was connected with Cu-NF 25 KV / 20 mA tube as a CuKα radiation source to record the diffractograms in the 2θ range 0–80°.

2.5.3. In-vitro drug permeation

From the abdominal region of healthy albino rats (150–200 g), the hair was carefully taken out without injury to the skin and then it was

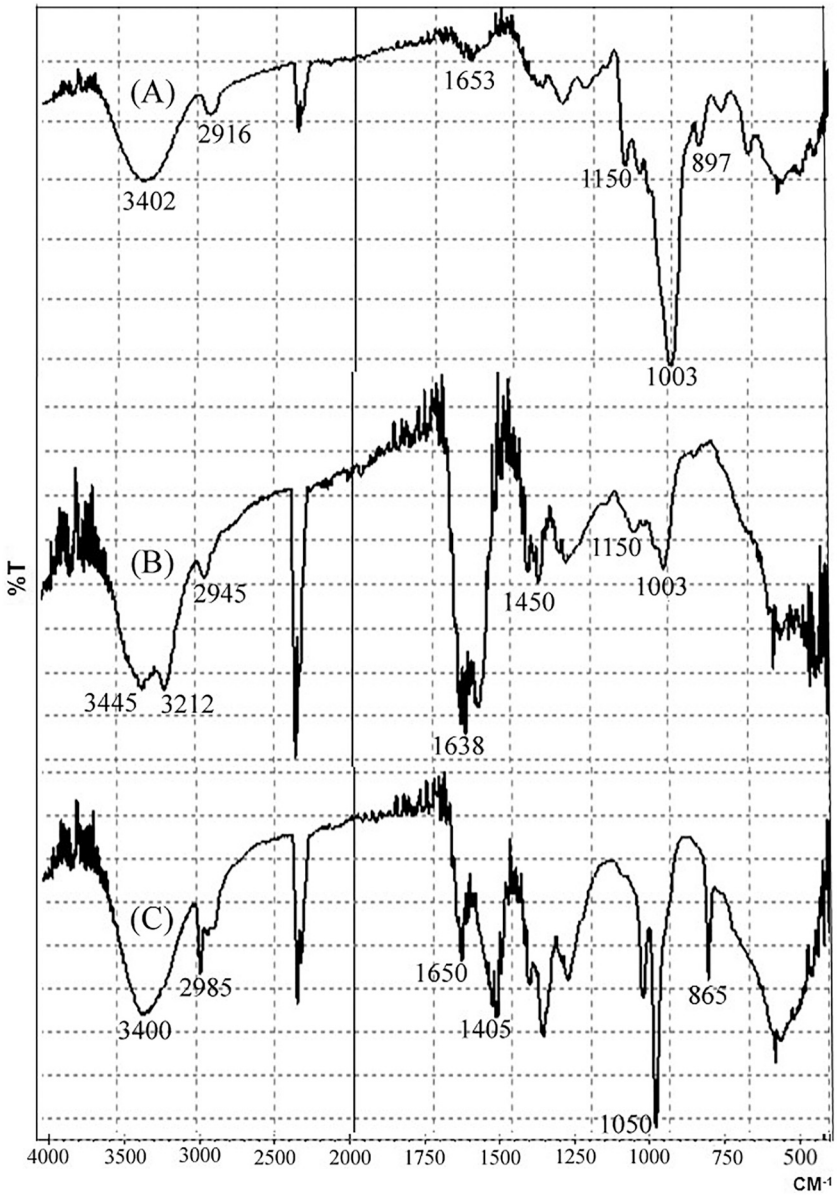

Fig. 2. FTIR spectra of Dxt (A), PAAm-g- Dxt (B) and hydrolyzed PAAm-g- Dxt (C).

Table 2
Results of neutralization equivalent and elemental analysis.

Polymer	NE	Elemental analysis		
		N (%)	C (%)	H (%)
DXT	1329.78	0.00	39.27	7.15
PAAm-g- Dxt	1220.40	14.22	42.16	9.59
Hydrolyzed PAAm-g- Dxt	496.17	4.28	28.72	6.50

excised. Any blood vessels or tissue adhering to the dermal side was carefully cleaned; the stratum corneum side was placed with ETDS and fixed with donor compartment of the cell through an adhesive. The study utilizes a Keshary-Chien diffusion cells, a receptor medium of pH 7.4 buffer solution with a magnetic stirrer set at 100 RPM with the entire assembly maintained at 32 °C ± 5 °C. The donor compartment inserted with a carbon anode was fixed on the receptor compartment having carbon cathode and were connected with a regulated DC power source for electric current. At specific intervals, 5 ml of sample were withdrawn for 24 h; the sampling volume was equally compensated by adding an equal buffer. The drug permeation was calculated with the help of UV–Visible spectrophotometer (Model UV-1800, Shimadzu, Japan) at 264 nm. The permeation study was performed with the following parameters: (a) without electric current, (b) with electric current (2, 4, and 8 mA) and (c) with 'on–off' electric current. This experimentation was endorsed by the institutional ethics committee (BLDE/BPC/Ph.D-01/2017–18. Dtd. 29-07-2017).

2.5.4. Histopathological evaluation of skin

The skin samples meant to be subjected for study using electric and without electric current were conserved in 10% buffered formalin solution after washing with normal saline. Ethyl alcohol in concentration of ascending degree (70, 80, 90, 96, and 99%) was used to dehydrate the samples and were cleared in xylene before embedding in paraffin. A 5 mm thick paraffin sections stained with hematoxylin-eosin, were used for histopathological examination under binocular light microscope and then photographed (Pillai and Panchagula, 2003).

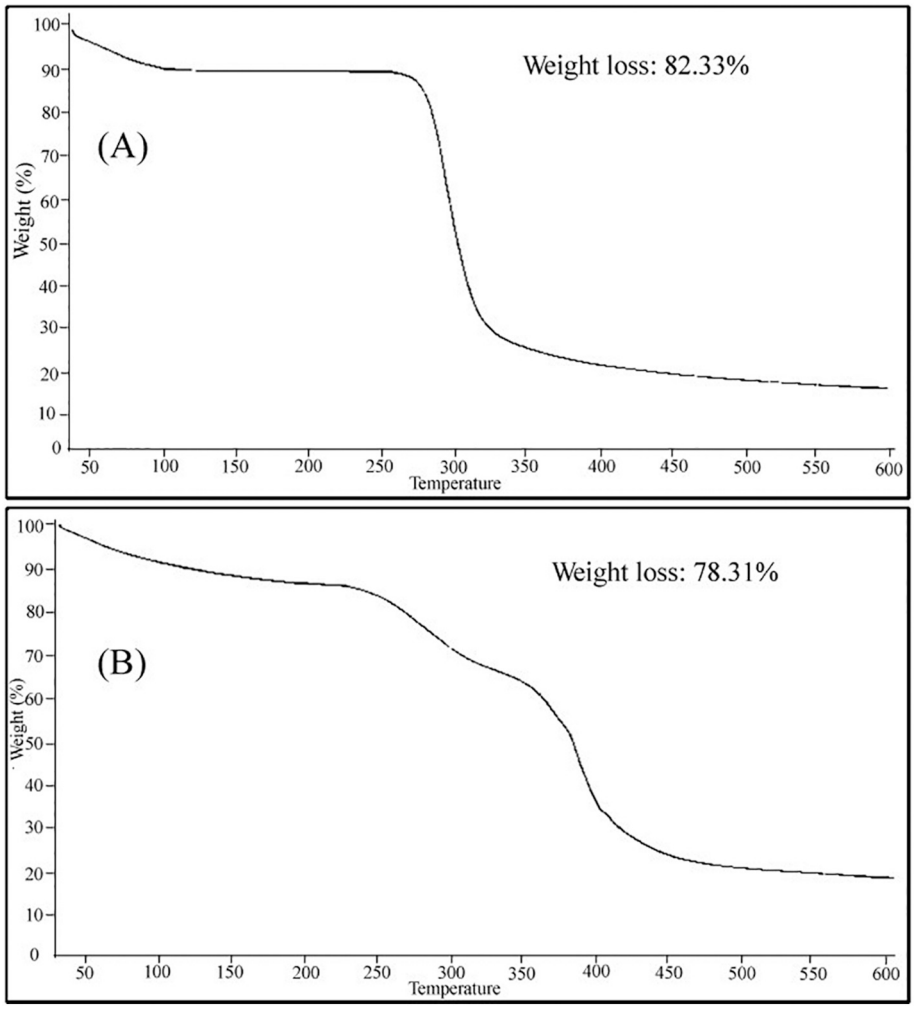

Fig. 3. TGA thermograms of Dxt (A) and PAAm-g- Dxt copolymer (B).

Table 3
Drug content & pH of hydrogel reservoir and thickness of RCM.

Formulations	Hydrogel reservoir		Thickness of RCM (μ)
	Drug content (%)	pH	
DXT1	87.35 ± 1.12	6.61	47 ± 0.98
DXT2	89.51 ± 1.21	6.72	48 ± 0.87
DXT3	93.28 ± 1.07	6.78	51 ± 0.79
DXT4	95.65 ± 1.27	6.68	53 ± 0.69
DXT5	95.03 ± 1.16	6.91	55 ± 1.05
DXT6	94.45 ± 1.49	6.79	70 ± 1.12
DXT7	93.42 ± 1.21	6.81	82 ± 0.93
DXT8	93.06 ± 1.27	6.71	89 ± 1.08

3. Results and discussion

A nitrogen atmosphere based free radical polymerization approach was employed to graft acrylamide (AAm) on the backbone of Dxt; partial hydrolysis of the PAAm-g-Dxt was carried out in the presence of NaOH solution, where the copolymer undergo saponification with the switching over of $–CONH_2$ groups to –COOH groups. The possible mechanism is explained in Scheme 1. The % grafting efficiency was 93.55% and % acrylamide grafting was found to be 85.47%.

3.1. Characterization of PAAm-g-Dxt copolymer

Fig. 1 shows the ^{1}HNMR of native Dxt (A), AAm (B) and PAAm-g-Dxt (C). In case of native Dxt, signals between 4 and 5 ppm are due to 3 and 6-linked-α-D-glc*p* residues, the signals between 3 and 4 ppm are because of protons in C2, C3, C4, C5 and C6. The signal appearing at 2.5 ppm is due to DMSO which was used as solvent. In the case of AAm, the signals at 5.6 and 6.1 ppm are related to CH_2 and CH protons, signals at 7.2 and 7.6 ppm are because of $CONH_2$ protons of AAm and

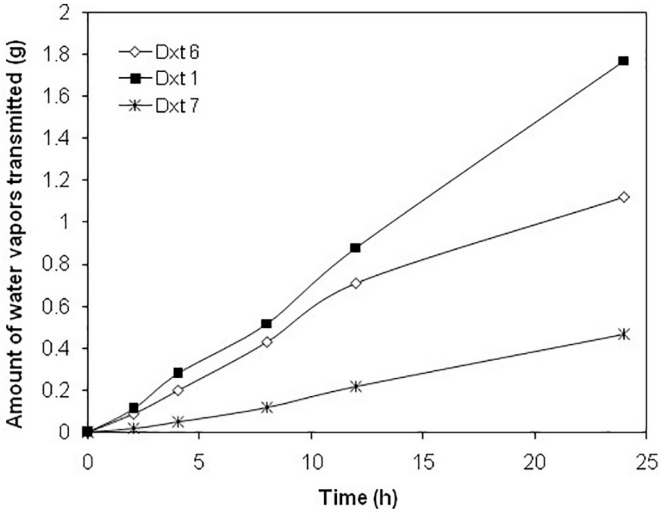

Fig. 4. Water vapor transmission profiles of rate controlling membranes.

Table 4
Tensile strength of rate controlling membranes.

RCM	Tensile strength (kg/cm^2)	Extension (mm)
Dxt1	0.146	38.96
Dxt6	0.208	37.24
Dxt7	0.394	6.62
Dxt8	0.556	1.65

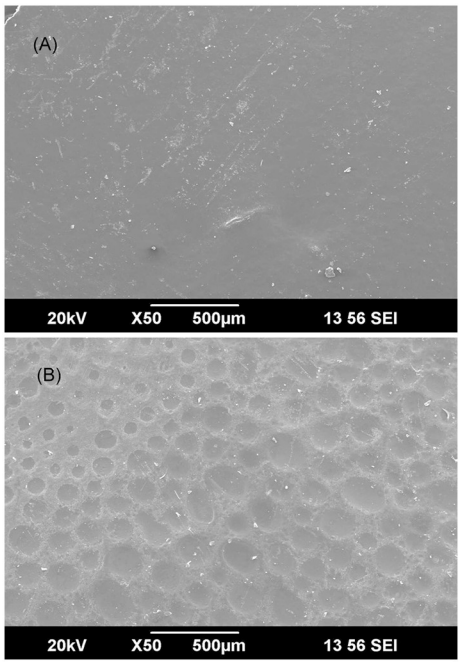

Fig. 5. SEM photographs of Dxt1 (A) and Dxt6 membranes (B).

signal at 2.5 ppm is due to DMSO. But for PAAm-g-Dxt copolymer, apart from the signals of Dxt, new signals at 1.5, 2.2 and 7.0 ppm were seen. The signal at 1.5 and 2.2 ppm are due to CH_2 and CH protons of PAAm and the signal centered at 7.0 ppm is because of $CONH_2$ protons of PAAm. Such results were also seen for polyacrylamide-g-poly(vinyl alcohol) copolymer (Demchenko et al., 2005). This corroborates the grafting reaction of PAAm on dextran.

Fig. 2 displays FTIR spectra of Dxt, PAAm-g-Dxt and hydrolyzed PAAm-g-Dxt. In the spectrum of Dxt, the hydroxyl stretching vibration was caused by the band nearly at 3402 cm^{-1}. The carbonyl group deformation was noted at band 1653 cm^{-1}. The stretch vibration of alcoholic hydroxyl groups was seen at bands 1150 cm^{-1} and 1003 cm^{-1}. The C—H stretch of aldehyde was recorded at band 2916 cm^{-1} and the band at 897 cm^{-1} was caused by α-glucopyranose ring deformation. In the spectrum of PAAm-g-Dxt, the peak related to —OH group stretch appeared at 3445 cm^{-1} and that of —NH stretch was observed at ~3212 cm^{-1}. The primary amide groups on the back bone of Dxt contributed two peaks at 1638 and 1450 cm^{-1}. The aliphatic stretch vibrations (—CH) was seen at 2945 cm^{-1} and alcoholic hydroxyl groups stretch vibration bands were observed at 1150 cm^{-1} and 1003 cm^{-1} respectively. The band at 897 cm^{-1} is due to α-glucopyranose ring deformation. Hence, this is the substantiation for grafting reaction. While in hydrolyzed PAAm-g-Dxt, the peak noted at 3400 cm^{-1} is related to the —OH groups, the peak at 2985 cm^{-1} was caused by the aliphatic –CH stretching vibration, the peak at 1650 cm^{-1} is attributed to the primary amide groups on Dxt,COO^- groups peak was observed at 1405 cm^{-1}. However, the peak emerged at ~3212 cm^{-1} in the spectra of PAAm-g-Dxt is disappeared indicating the partial hydrolysis of grafted copolymer.

Table 2 depicts the data of elemental analysis. A 0.00% of nitrogen,

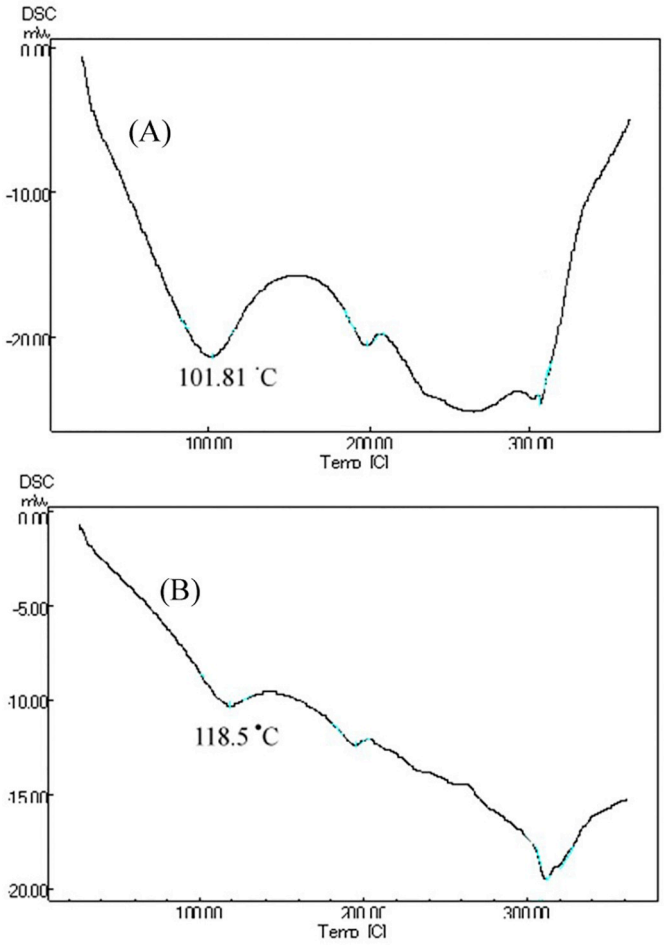

Fig. 6. DSC thermograms of Dxt1 (A) and Dxt6 (B) membranes.

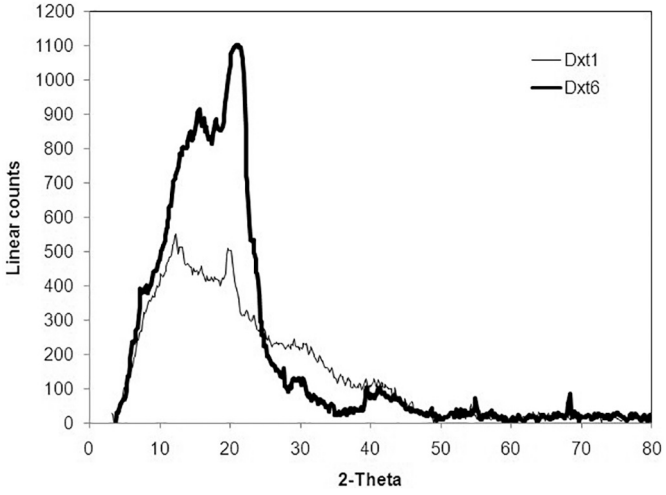

Fig. 7. X-ray diffractograms of Dxt1 and Dxt6 membranes.

39.27% carbon and 7.15% hydrogen were seen with native Dxt, but the PAAm-g-Dxt copolymer is reported to have 14.22% of nitrogen, 42.16% carbon and 9.59% hydrogen; the significant enhancement in nitrogen content could be because of–$CONH_2$ groups presence on the Dxt backbone post grafting. Whereas, with hydrolyzed PAAm-g-Dxt, we observed 4.28% of nitrogen, 28.72% carbon and 6.50% hydrogen. In the hydrolyzed copolymer, the change of —$CONH_2$ groups to —COOH groups resulted in decreased nitrogen content to 4.28%, which confirms

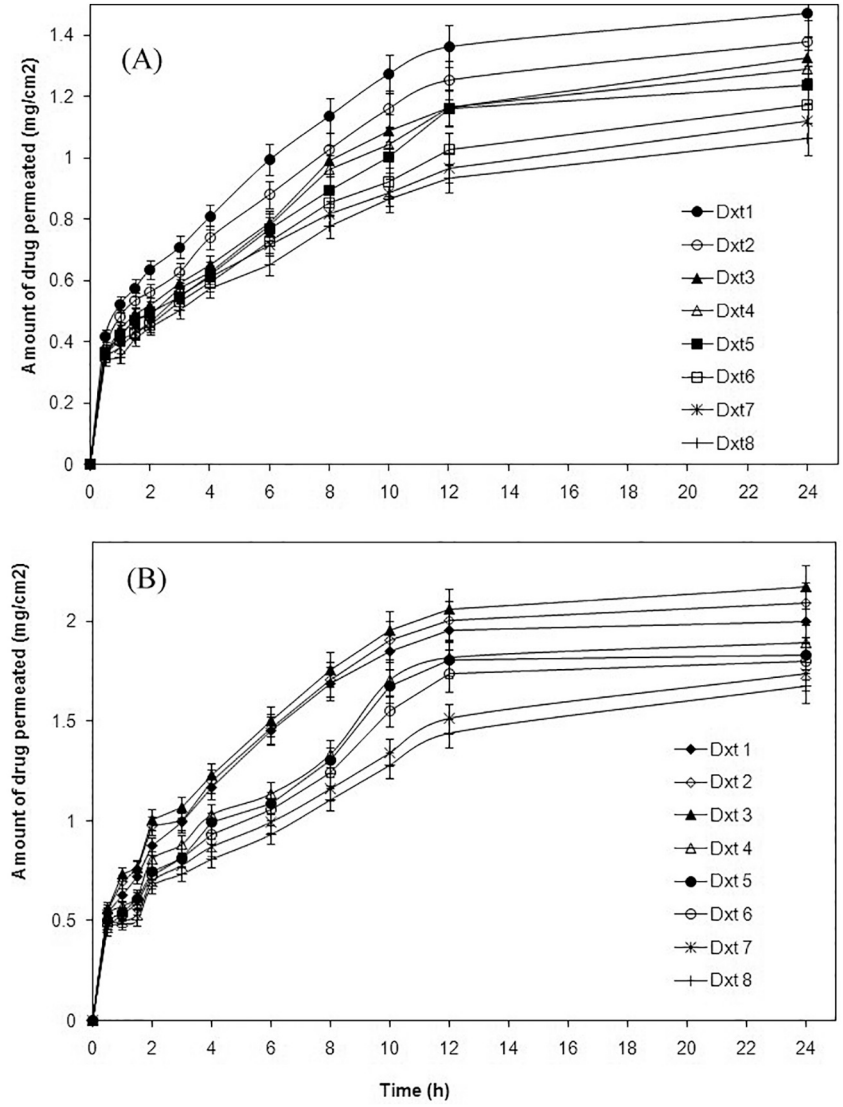

Fig. 8. In vitro drug permeation profiles without electric stimulus (A) and with applied electric stimulus (B) through rat skin.

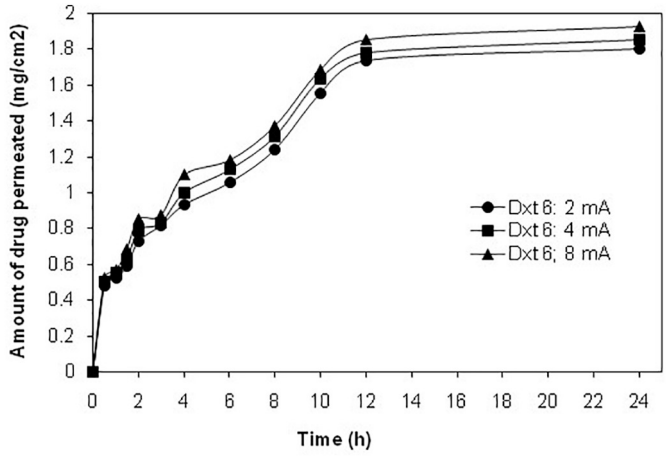

Fig. 9. Effect of electric current strength on drug permeation through rat skin.

the grafting and alkaline hydrolysis. Such results also reported earlier (Kulkarni and Sa, 2009).

The neutralization equivalent values (NE) of Dxt, PAAm-g-Dxt and hydrolyzed PAAm-g-Dxt were 1329.78 MEq/g, 1220.40 MEq/g and 496.17 MEq/g respectively (Table 2). This indicates that the hydrolysed PAAm-g-Dxt carries large carboxyl groups than the un-grafted Dxt and these carboxyl groups are held responsible for electrical-responsivity of grafted copolymer.

Fig. 3 shows the TG analysis of Dxt and PAAm-g-Dxt. With Dxt, the degradation was noted after 200 °C and 9.94% weight loss was seen up to 200 °C because of loss of bound and unbound moisture from Dxt. Further, 72.38% weight loss was observed from 200 to 400 °C and finally a value of 82.33% weight loss at 600 °C possibly due to decomposition of Dxt. But, for PAAm-g-Dxt, the weight loss (12.88%) was observed in the range of 25 to 200 °C. In between 200 and 400 °C, 65.44% weight loss was recorded which finally reaches to 78.31% at 600 °C.We have observed a steady mass loss for PAAm-g-Dxt copolymer and percent residual weight of PAAm-g-Dxt was greater (21.69%) than the native Dxt (17.67%). This shows the improved thermal stability of PAAm-g-Dxt graft copolymer as compared to native Dxt. The grafted copolymer has characteristics of both natural and synthetic polymers with adequate strength and thermal stability (Alange et al., 2017). This proves the graft copolymer formation.

3.2. Evaluation of ETDS

The developed reservoir hydrogels were evaluated for pH and drug

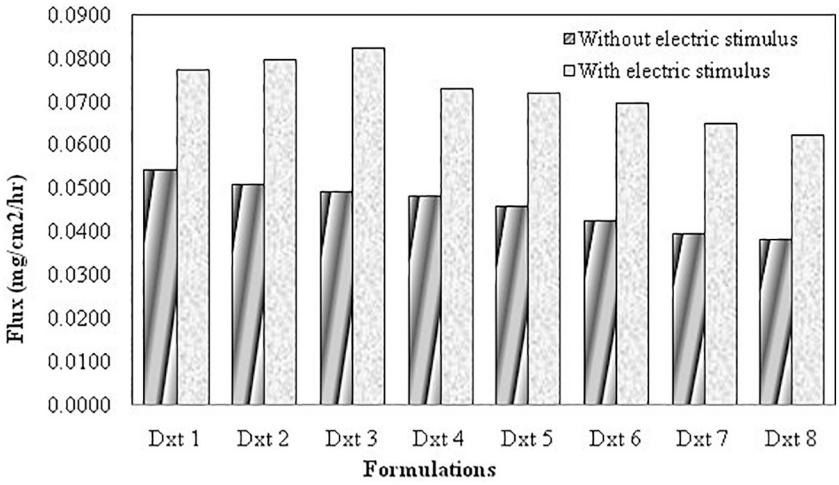

Fig. 10. Flux values obtained from drug permeation in the absence or presence of electric stimulus.

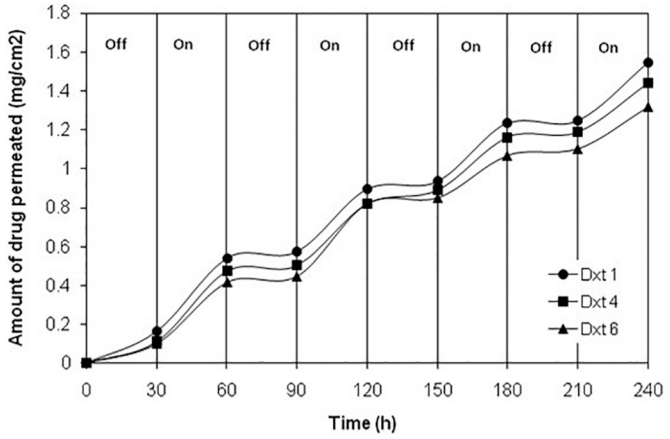

Fig. 11. Pulsatile release behavior of ETDDS, in which electric stimulus was switched on and off at 30 min time intervals.

Table 5
Flux (*Jss*), permeability coefficients (*Pm*), and enhancement factors (*EF*).

Formulations	Without electric stimulus		With electric stimulus		
	Jss (mg/cm^2/h)	Pm (mg/h.cm)	Jss (mg/cm^2/h)	Pm (mg/h.cm)	EF
DXT1	0.0543	0.0139	0.0774	0.0198	1.426
DXT2	0.0511	0.0130	0.0796	0.0203	1.557
DXT3	0.0493	0.0126	0.0824	0.0210	1.672
DXT4	0.0484	0.0123	0.0730	0.0186	1.509
DXT5	0.0460	0.0117	0.0721	0.0184	1.565
DXT6	0.0427	0.0109	0.0699	0.0178	1.638
DXT7	0.0397	0.0101	0.0650	0.0166	1.635
DXT8	0.0382	0.0097	0.0624	0.0159	1.633

Jss: Flux (mg/cm^2/h), *Pm*: Permeability coefficient (mg/h.cm), *EF*: Enhancement factor.

content. The gels were uniform and translucent; pH was in the range of 6.61 to 6.91, which falls in the normal pH range of skin and drug content was found to be 87.35 to 95.65% (Table 3).

The prepared RCMs were smooth, thin and flexible. The technique employed for casting the RCMs on glass plate was found suitable. The thickness was in the range of 47 to 89 μ; it increased with increase in concentration of GA (Table 3). The WVT through RCM determines the drug permeability characteristics. The rate of WVT of RCMs was affected by the concentration of GA; greater the concentration GA, lower was the WVT rate (Fig. 4). The tensile strengths of the RCMs are given in Table 5. The Dxt1, Dxt6, Dxt7 and Dxt8 membranes have shown a tensile strength of 0.146, 0.208, 0.394 and 0.556 kg/cm^2 respectively (Table 4). The study indicated that, the tensile strength increases with increase in the concentration of GA due to increased stiffness of membranes.

Scanning electron microscopy was performed to know the effect of crosslinking on the surface structure of RCMs. The SEM photographs presented in Fig. 5 reveal that the Dxt6 RCM has demonstrated rough and dense surface than Dxt1. As the concentration of GA increases, the membranes undergo shrinkage leading to rough and dense surface. The DSC thermograms of Dxt1 and Dxt6 RCMs are presented in Fig. 6. The Dxt1 membrane has shown an endothermic peak at 101.81 °C. Whereas Dxt6 membrane has shown an endothermic peaks at 118.5 °C. This increase in endothermic peak with Dxt6 membrane indicates the increased membrane toughness due to increased concentration of GA. The X-ray diffractograms of Dxt1 and Dxt6 RCMs are seen in Fig. 7. The Dxt1 membrane has shown characteristic intense peaks between the 2θ of 5° and 20°. Whereas, in case of Dxt6 membranes, intense peaks were seen between 2θ of 5° and 30°. However, the peak intensity with Dxt6 is high as compared to that of Dxt1. This may be due to increased crosslinking agent, GA in the membranes.

3.3. In-vitro drug permeation

The permeation profiles of ETDS in the absence or presence of electric current are presented in Figs. 8–11. The permeation of drug in the absence of electric current was slow as against permeation rate under electric stimulus. We noticed that the permeation enhancement was reliant on the density of applied electric current.

In the absence of electric current, small amount of drug permeation was seen. A maximum of 66.09% of drug has got permeated at end of 24 h from Dxt1 formula. But, as the concentration of PAAm-g-Dxt was enhanced, the drug permeation got decreased, which may be due to increased viscosity of gel. While, increased amount of GA resulted in decreased drug permeation; this may be attributed to increased stiffness of the membrane that leads to reduced pore size resulting in diminished drug permeation (Fig. 8A).

While, in the presence of electric current of 2 mA, the permeability rate of drug was increased as compared to drug permeation without electric current (Fig. 8B). About 1.6 fold increase in flux was noticed with the application of DC electric current. A maximum drug permeability of 97.54% was recorded at the end of 24 h from Dxt3 formulation; this may be due to electric responsiveness of the hydrogel reservoir with enhanced concentration of PAAm-g-Dxt copolymer. Under

Table 6
Histopathology of normal skin and skin treated with electric stimulus (2 mA).

Sl. no	Parameters	Normal skin	Skin treated with electric stimulus (2 mA)
01	Stratum corneum intactness	1	2
02	Epidermis liquification	0	2
03	Subepidermal odema	0	2
04	Collagen fiber swelling	0	3
05	Inflammatory cell infiltrate	0	0
06	Skin appendages degeneration	0	2

Scores: 0 - No Change, 1 – Very Light Change, 2 – Slight Change, 3– Moderate Change, 4 – Marked Change.

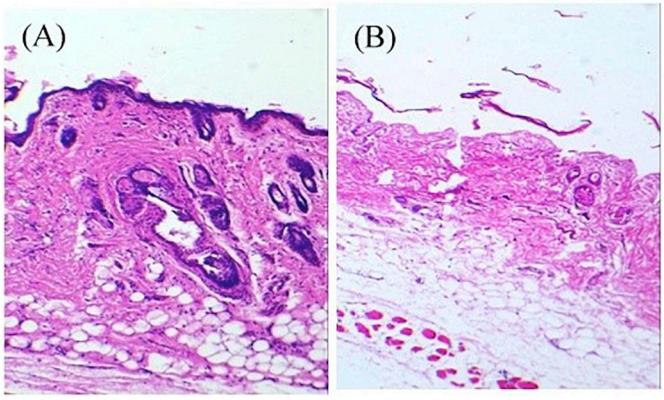

Fig. 12. Histopathology of rat skin before (A) and after application of electrical stimulus (B) (Hematoxylin-Eosin, 100×).

applied DC current, a considerable increase in drug permeation was recorded. The drug permeation tends to decrease with increased concentration of GA in the RCM and hydrogel reservoirs (Fig. 8A). An increase in the permeation rate was observed with increasing electric current from 2 to 8 mA (Fig. 9).

The calculated steady state flux (Jss) and the permeability coefficient (Kp) values are shown in Table 5 and Fig. 10 using the formula:

$$Kp = Jss/Cv \quad (4)$$

where Cv is total drug concentration in donor compartment.

The enhancement factors (*EF*) were found to be between 1.426 and 1.672 as computed using the relation:

$$EF = Jss \text{ with electric current}/Jss \text{ without electric current} \quad (5)$$

The applied electric current has improved the drug permeability rate through rat skin. The flux values determined in the absence of electric current were in the range of 0.0382 to 0.0543 mg/cm^2/h, but the flux values for permeation with electric current were greater and were in the range of 0.0624 to 0.0824 mg/cm^2/h (Fig. 10).

In order to confirm the electrical responsiveness of ETDS, the drug permeation study was also conducted under “on–off” electric stimulus pattern and presented in Fig. 11. Under applied electric current, (“ON”) the higher permeation was noticed and permeation got decreased when electric current was switched ‘off.’When electric current was applied to the negatively charged PAAm-g-Dxt hydrogel, the counterion of polyion travels close to negative electrode. The polyion is static and other free ions in the hydrogel move towards counter electrodes across hydrogel. This builds dissimilarity in osmotic pressure in the hydrogel and it acts as driving force for drug release from hydrogel (Kim and Lee, 1999).

3.4. Histopathological evaluation of skin

The Table 6 and Fig. 12 show the changes in the structure of skin before and after application of electrical current. The stratum corneum of the normal skin in the absence of electrical current tends to be intact with preserved structural integrity and without inflammatory cell infiltration or alteration in the skin appendages and there were no subepidermal edema and collagen fiber swelling. But, for skin sample with electric current, slight alteration in the intactness of stratum corneum were noticed; the cell structural integrity was loosened with sub-epidermal edema and collagen fiber swelling and there was a degeneration of skin appendages. Transdermal permeability is a complex mechanism; it is difficult to understand by which mechanism the permeability increases. Through histopathology studies, we can analyze the anatomy of skin before and after application of electric stimuli. In this study, we observed certain reversible changes in the skin structure after application of electric stimulus; this might have resulted in enhanced drug permeation through skin.

4. Conclusion

The electro-responsive PAAm-g-Dxt copolymer was successfully synthesized through nitrogen atmosphere based free-radical polymerization and characterized by ^{1}HNMR & FTIR spectroscopy, elemental and TG analysis to ascertain the grafting reaction. The ETDS were developed utilizing drug-loaded PAAm-g-Dxt hydrogel as the reservoir, and cross-linked Dxt-PVA blend films as RCM. In the absence of electrical stimuli, little drug was permeated, while in the presence of electrical stimuli; the drug permeability was increased. About 1.6 fold increased flux was recorded. As the concentration of GA was increased, the drug permeability was decreased. But, the drug permeability rate was increased when the strength of applied electric current was increased from 2 to 8 mA. The histopathology study confirmed the altered skin structural integrity after application of electrical stimuli. Hence, the PAAm-g-Dxt copolymer is useful biomaterial for successful development of ETDS triggered by an electric stimulus to supply on-demand drug into the body.

Acknowledgements

Authors express sincere thanks to authorities at BLDE Association, Vijayapur, Karnataka, India for supporting this work.

References

Alange, V.V., Birajdar, R.P., Kulkarni, R.V., 2017. Functionally modified polyacrylamide-graft-gum karaya pH-sensitive spray dried microspheres for colon targeting of an anti-cancer drug. Int. J. Biol. Macromol. 102, 829–839.
Amiri, S., Ramezani, R., Aminlari, M., 2008. Antibacterial activity of dextran-conjugated lysozyme against *Escherichia coli* and *Staphylococcus aureus* in cheese curd. J. Food Protect. 71, 411–415.
Aziz, M.A., Cabral, J.D., Brooks, H.J.L., Moratti, S.C., Hanton, L.R., 2012. Antimicrob. Agents Chemother. 56, 280–287.
Bankova, M., Manolova, N., Markova, N., Radoucheva, T., Dilova, K., Rashkov, I., 1997. Hydrolysis and antibacterial activity of polymers containing 8-quinolinyl acrylate. J. Bioact. Compat. Polym. 12, 294–307.
Birks, J., Grimley, E.J., Iakovidou, V., Tsolaki, M., 2000. Rivastigmine for alzheimer's. disease. Cochrane Database Syst. Rev. 4, CD001191.
Boppana, R., Kulkarni, R.V., Krishna Mohan, G., Mutallik, S., Aminabhavi, T.M., 2016. In-vitro and in-vivo assessment of novel pH-sensitive interpenetrating polymer networks of graft copolymer for gastro-protective delivery of ketoprofen. RSC Adv. 6, 64344–64356.
Chauhan, A., Kaith, B.S., Singha, A.S., Pathania, D., 2010. Induction of the morphological changes in *hibiscus sabdariffa* on graft copolymerization with acrylonitrile and co-vinyl monomer in binary mixtures. Malaysian Polym. J. 52, 140–150.
Demchenko, O., Zheltonozhskaya, T., Turov, A., Tsapka, M., Syromyatnikov, V., 2005. Poly(vinyl alcohol)-*graft*-polyacrylamide with different grafts number and length as studied by ^{1}HNMR spectroscopy. Mol. Cryst. Liq. Cryst. 427, 225–233.
Flory, P.J., 1950. Statistical mechanics of swelling of network structures. J. Chem. Phys. 18, 108–111.
Flory, P.J., Rehner, J., 1943. Statistical mechanics of cross-linked polymer networks. II. Swelling. J. Chem. Phys. 11, 521–526.

Gorle, A.P., 2016. A way to increase effectiveness of paracetamol drug through transdermal patch. Int. J. Pharm. 7, 30–35.
Hennik, W.E., De Jong, S.J., Bos, G.W., Veldhuis, T.F.J., Van Nostrum, C.F., 2004. Biodegradable dextran hydrogels crosslinked by stereocomplex formation for the controlled release of pharmaceutical proteins. Int. J. Pharm. 277, 99–104.
Hickey, A.S., Peppas, N.A., 1995. Mesh size and diffusive characteristics of semi-crystalline poly(vinyl alcohol) membranes prepared by freezing/thawing techniques. J. Membr. Sci. 107, 229–237.
Kim, S.Y., Lee, Y.M., 1999. Drug release behavior of electrical responsive poly(vinylalcohol)/poly(acrylic acid) IPN hydrogels under an electric stimulus. J. Appl. Polym. Sci. 74, 1752–1761.
Kulkarni, R.V., Sa, B., 2008. Enteric delivery of ketoprofen through functionally modified poly(acrylamide-grafted-xanthan) based pH-sensitive hydrogel beads: preparation, in-vitro and in-vivo evaluation. J. Drug. Target. 16, 167–177.
Kulkarni, R.V., Sa, B., 2009. Polyacrylamide-grafted-alginate-based pH-sensitive hydrogel beads for delivery of ketoprofen to the intestine: in vitro and in vivo evaluation. J. Biomater. Sci. Polym. Edn. 20, 235–251.
Kumari, A., Kaith, B.S., Singha, A.S., Kalia, S., 2010. Synthesis, characterization and salt resistance swelling behavior of psy-g-poly (AA) hydrogel. Adv. Mater. Lett. 1, 123–128.
Lee, S.B., Koepsel, R.R., Morley, S.W., Matyjaszewski, K., Sun, Y., Russell, A.J., 2004. Permanent, non-leaching antibacterial surfaces. 1. Synthesis by atom transfer radical polymerization. Bio-macromolecules 5, 877–882.
Le'Vesque, S.G., Lim, R.M., Shoichet, M.S., 2005. Macroporous interconnected dextran scaffolds of controlled porosity for tissue-engineering applications. Biomaterials 26, 7436–7446.
Manikkath, J., Manikkath, A., Shavi, G.V., Bhat, K., Mutalik, S., 2017. Low frequency ultrasound and PAMAM dendrimer facilitated transdermal delivery of ketoprofen. J. Drug Del. Sci.Tech. 41, 334–343.
Mutalik, S., Udupa, N., 2005. Formulation development, in-vitro and in-vivo evaluation of membrane controlled transdermal systems of glibenclamide. J. Pharm. Pharmaceut. Sci. 8, 26–38.
Oh, S.T., Han, S.H., Ha, C.S., Cho, W.J., 1996. Synthesis and biocidal activities of polymer. IV. Antibacterial activity and hydrolysis of polymers containing diphenyl ether. J. Appl. Polym. Sci. 59, 1871–1878.
Peppas, N.A., 1997. Hydrogels and drug delivery. Curr. Opin. Coll. Int. Sci. 2, 531–537.
Peppas, N.A., Langer, R., 1994. New challenges in biomaterials. Science 263, 1715–1720.
Peppas, N.A., Merrill, E.W., 1976a. PVA hydrogels: reinforcement of radiation-crosslinked networks by crystallization. J. Polym. Sci. Polym. Chem. Ed. 14, 441–457.
Peppas, N.A., Merrill, E.W., 1976b. Differential scanning calorimetry of crystallized PVA hydrogels. J. Appl. Polym. Sci. 20, 1457–1465.
Peppas, N.A., Mongia, N.K., 1997. Ultrapure poly(vinyl alcohol) hydrogels with mucoadhesive drug delivery characteristics. Eur. J. Pharm. Biopharm. 43, 51–58.
Pillai, O., Panchagula, R., 2003. Transdermal delivery of insulin from poloxamer gel: ex vivo and in vivo skin permeation studies in rat using iontophoresis and chemical enhancers. J. Control. Release 89, 127–140.
Ratner, B.D., Hoffman, A.S., 1976. Synthetic hydrogels for biomedical applications. In: Andrade, J.D. (Ed.), Hydrogels for Medical and Related Applications, ACS Symposium Series, No. 31. American Chemical Society, Washington, DC, pp. 1–36.
Sharma, A.K., Mishra, A.K., 2010. Microwave assisted synthesis of chitosan-graft styrene for efficient Cr (VI) removal. Adv. Mater. Lett. 1, 59–69.
Stauffer, S.R., Peppas, N.A., 1992. Poly(vinyl alcohol) hydrogels prepared by freezing-thawing cyclic processing. Polymer 33, 3932–3936.
Tiller, J.C., Lee, S.B., Lewis, K., Klibanov, A.M., 2002. Polymer surfaces derivatized with poly(vinyl-N-hexylpyridinium) kill airborne and waterborne bacteria. Biotechnol. Bioeng. 79, 465–471.
Tripathy, T., Singh, R.P., 2000. High performance flocculating agent based on partially hydrolysed sodium alginate-g-polyacrylamide. Eur. Polym. J. 36, 1471–1476.